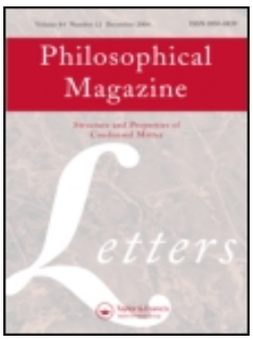

Philosophical Magazine Letters

ISSN: 0950-0839 (Print) 1362-3036 (Online) Journal homepage: https://www.tandfonline.com/loi/tphl20

Analytical contrast factor of dislocations along orthogonal diad axes

J. Martinez-Garcia , M. Leoni & P. Scardi

To cite this article: J. Martinez-Garcia , M. Leoni & P. Scardi (2008) Analytical contrast factor of dislocations along orthogonal diad axes, Philosophical Magazine Letters, 88:6, 443-451, DOI: 10.1080/09500830802159075

To link to this article: https://doi.org/10.1080/09500830802159075

Philosophical Magazine Letters
Vol. 88, No. 6, June 2008, 443–451

Taylor & Francis
Taylor & Francis Group

Analytical contrast factor of dislocations along orthogonal diad axes

J. Martinez-Garcia, M. Leoni and P. Scardi*

Department of Materials Engineering and Industrial Technologies, University of Trento, Trento, Italy

(*Received 22 February 2008; final version received 21 April 2008*)

An analytical expression valid for any crystal system is proposed for the diffraction contrast factor of dislocations lying along a diad axis with another diad perpendicular to it. This symmetry requirement is common to several slip systems in real materials, for which the proposed solution can provide a direct relationship between diffraction line broadening, dislocation slip system and elastic properties. As an example of the utility of the contrast factor in analytical form, the main slip system of Fluorite-type structures $\langle 1\bar{1}0\rangle\{001\}$ is considered and the dependence of the line broadening anisotropy is shown as a function of the elastic anisotropy and Poisson's ratio.

Keywords: dislocations; contrast factor; WPPM; line profile analysis; X-ray diffraction

1. Introduction

X-ray diffraction (XRD), being sensitive to the local atomic arrangement, is frequently used to study deviations from the perfect crystalline order. This is of particular interest in the study of nanocrystalline and heavily deformed materials, where line profile analysis (LPA) can provide information on shape and size distribution of crystalline domains below ~1 μm, and lattice defects like, e.g. dislocations, faulting, misfitting inclusions and antiphase domains [1].

In recent years, traditional LPA methods based on the information from a few isolated XRD peak profiles (e.g. Williamson–Hall plot and Warren–Averbach method [2]), evolved towards full pattern approaches, like the whole powder pattern modelling (WPPM) [3,4], allowing the simultaneous analysis of virtually all line broadening sources in the entire powder diffraction pattern.

The theory of dislocation line broadening is based on the Krivoglaz–Wilkens model [5–8], according to which the Fourier Transform of the XRD peak profile is

$$A^D_{hkl} = \exp\left[-\frac{1}{2}\pi b^2 \bar{C}_{hkl}\rho d^{*2} L^2 f^*\left(\frac{L}{R_e}\right)\right] \tag{1}$$

*Corresponding author. Email: Paolo.Scardi@unitn.it

ISSN 0950–0839 print/ISSN 1362–3036 online

DOI: 10.1080/09500830802159075
http://www.informaworld.com

where L is the Fourier (or coherence) length, b is the Burgers vector modulus, ρ is the average dislocation density, R_e is the effective outer cut-off radius, d^* is the modulus of the scattering vector in Bragg condition ($\boldsymbol{d}^*$), and f^* is a known function of L/R_e [7].

$\bar{C}_{hkl}$ is the average contrast factor (the average being performed on all active slip systems for a random-oriented polycrystalline), accounting for the anisotropy of the dislocation strain field and of the elastic medium. Even though it can be demonstrated that, in the general case $\bar{C}_{hkl}$ can be written as a fourth-order invariant form of the Miller indices (hkl), coefficients of this invariant must be calculated numerically, given the information on unit cell parameters, Burgers vector and slip system, and elastic constants (c_{ij} or s_{ij}) [9–12].

So far, the need for a numerical procedure has critically limited our understanding of the relations between dislocation geometry, elastic anisotropy and diffraction line broadening. In a recent paper, we demonstrated that an analytical expression of $\bar{C}_{hkl}$ as a function of elastic anisotropy (Zener ratio), A_z and Poisson's ratio ν, can be written for the $\langle 001\rangle\{100\}$ cubic slip-system typical of Cu_2O [13]. In the present work, we show that a general expression can be written for the case of dislocations lying along a diad axis with a further diad axis perpendicular to it, a condition frequently observed in real slip systems (Table 1).

2. The analytical solution

In the most general form, the contrast factor for a given slip system can be written as [8,14]:

$$C = \frac{1}{\pi}\int_0^{\pi} \Psi^2(\varphi)\mathrm{d}\varphi \tag{2}$$

where φ is a rotation around the dislocation line, $\boldsymbol{l}$, [Figure 1(a)] and Ψ is related to the displacement field $\boldsymbol{u}$ of the dislocation:

$$\Psi^2(\varphi) = \frac{2\pi r}{b}\sum_i^3\sum_j^2(\hat{\boldsymbol{d}}^*\cdot\boldsymbol{e}_i)(\hat{\boldsymbol{d}}^*\cdot\boldsymbol{e}_j)\frac{\partial u_i}{\partial x_j}. \tag{3}$$

The $\boldsymbol{u}$ field can be written as a function of (x_1, x_2), coordinates in the $\{\boldsymbol{e}_1, \boldsymbol{e}_2\}$ plane, as:

$$\boldsymbol{u}(x_1, x_2) = 2\Re\mathrm{e}[\mathrm{A}\cdot\boldsymbol{f}(x_1, x_2)] \tag{4}$$

where $\boldsymbol{f}$ is a vector whose elements are given by the complex potential function $f_\alpha(x_1, x_2)$ $(\alpha = 1, 2, 3)$

$$f_\alpha(x_1, x_2) = -\frac{1}{4\pi l}\left(\frac{\boldsymbol{L}_\alpha\cdot\boldsymbol{b}}{\boldsymbol{A}_\alpha\cdot\boldsymbol{L}_\alpha}\right)\ln(x_1 + p_\alpha x_2). \tag{5}$$

The p_α terms are eigenvalues of the fundamental elasticity matrix $\mathbf{N}$ [15] for which $\Im\mathrm{m}(p_\alpha) > 0$, and $(\boldsymbol{A}_\alpha, \boldsymbol{L}_\alpha)$ their associated eigenvectors. In the formulae above, $\Re\mathrm{e}(x)$ and $\Im\mathrm{m}(x)$ denote, the real and imaginary part of the complex number x, respectively. The three vectors $\boldsymbol{A}_\alpha$ in column, form the $\mathbf{A}$ matrix in Equation (4).

Table 1. The dimensionless parameters ($\gamma^2, \gamma_0, \gamma_1, \lambda^4$) as function of the elastic constants for the most known diad-slip systems.

Slip systems	Screw γ^2	Edge γ_0	Edge γ_1	Edge λ^4	Examples
$\langle 001\rangle\{100\}^c$	1	$\frac{c_{12}}{c_{44}}$	$\frac{c_{11}}{c_{44}}$	1	Cu_2O and its isomorphs
$1/2\langle 1\bar{1}0\rangle\{001\}^c$	$\frac{(c_{11}-c_{12})}{2c_{44}}$	$\frac{c_{12}}{c_{44}}$	$\frac{c_{11}}{c_{44}}$	$\frac{(c_{11}+c_{12}+2c_{44})}{2c_{11}}$	Ionic crystals, fluorite structures
$1/2\langle 1\bar{1}0\rangle\{110\}^c$	$\frac{2c_{44}}{(c_{11}-c_{12})}$	$\frac{(c_{11}+c_{12}-2c_{44})}{(c_{11}-c_{12})}$	$\frac{(c_{11}+c_{12}+2c_{44})}{(c_{11}-c_{12})}$	1	Ionic crystals, non-stoichiometric spinels
$1/2\langle 1\bar{1}0\rangle\{111\}^c$	$\frac{(c_{11}-c_{12}+4c_{44})}{2(c_{11}-c_{12}+c_{44})}$	–	–	–	All f.c.c metals and alloys
$1/3\langle 2\bar{1}\bar{1}0\rangle\{0001\}^{h,t}$	$\frac{(c_{11}-c_{12})}{2c_{44}}$	$\frac{c_{13}}{c_{44}}$	$\frac{c_{33}}{c_{44}}$	$\frac{c_{11}}{c_{33}}$	All layer structures, Sb, Bi_2Te_3
$1/3\langle 0001\rangle\{1\bar{1}00\}^{h,t}$	1	$\frac{c_{13}}{c_{44}}$	$\frac{c_{11}}{c_{44}}$	$\frac{c_{33}}{c_{11}}$	Be, BeO
$1/3\langle 2\bar{1}\bar{1}0\rangle\{01\bar{1}0\}^{h,t}$	$\frac{2c_{44}}{(c_{11})-c_{12}}$	–	–	–	TiB_2, WC, Ti, Zr

(*continued*)

Table 1. Continued.

Slip systems	Screw γ^2	Edge γ_0	Edge γ_1	Edge λ^4	Examples
$1/3\langle 2\bar{1}\bar{1}0\rangle\{10\bar{1}1\}^{h}$	$\dfrac{\left[\dfrac{3}{4}+\dfrac{2\kappa c_{44}}{(c_{11}-c_{12})}\right]}{\left[\kappa+\dfrac{3c_{44}}{2(c_{11}-c_{12})}\right]}$	–	–	–	Be
$\langle 100\rangle\{001\}^{te}$	$\dfrac{c_{66}}{c_{44}}$	$\dfrac{c_{13}}{c_{44}}$	$\dfrac{c_{33}}{c_{44}}$	$\dfrac{c_{11}}{c_{33}}$	Rutile/Cassiterite structures, Sn
$\langle 001\rangle\{110\}^{te}$	1	$\dfrac{c_{13}}{c_{44}}$	$\dfrac{(c_{11}+c_{12}+2c_{66})}{2c_{44}}$	$\dfrac{2c_{33}}{(c_{11}+c_{12}+2c_{66})}$	Rutile/Cassiterite structures, Sn
$[010](001)^{o}$	$\dfrac{c_{66}}{c_{44}}$	$\dfrac{c_{23}}{c_{44}}$	$\dfrac{c_{33}}{c_{44}}$	$\dfrac{c_{22}}{c_{33}}$	Perovskite structures, Ga
$[100](010)^{o}$	$\dfrac{c_{55}}{c_{66}}$	$\dfrac{c_{12}}{c_{66}}$	$\dfrac{c_{22}}{c_{66}}$	$\dfrac{c_{11}}{c_{22}}$	Mg_2SiO_4, $\alpha-U$

Note: The superscripts c, h, t, te, o denote the cubic, hexagonal, trigonal, tetragonal and orthorhombic crystal systems, respectively, and $\kappa=(c/a)^2$.

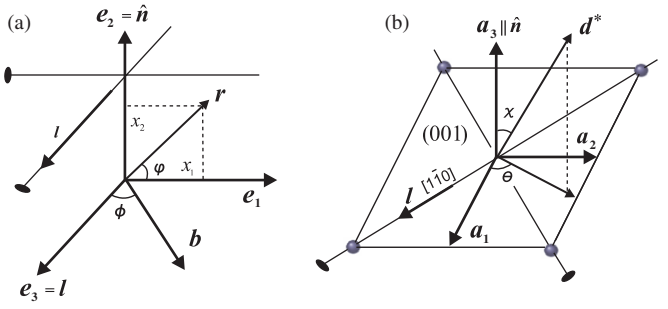

Figure 1. Schematic representation of a dislocation line along orthogonal diad axes. (a) A diad dislocation ($\boldsymbol{l}$, $\boldsymbol{b}$) of character ϕ and its slip system $\{\boldsymbol{e}_1, \boldsymbol{e}_2, \boldsymbol{e}_3\}$. (b) The $\langle 1\bar{1}0\rangle\{001\}$ slip system and the (θ, χ) angles of the scattering vector $\boldsymbol{d}^*$ with respect to the crystal basis$\{\boldsymbol{a}_1, \boldsymbol{a}_2, \boldsymbol{a}_3\}$.

When $\boldsymbol{l}$ is along a diad axis with a further diad perpendicular to it (Figure 1), $\mathbf{N}$ takes the following simple form:

$$\boldsymbol{N} = \begin{bmatrix} 0 & -1 & 0 & \frac{1}{c'_{66}} & 0 & 0 \\ -\frac{c'_{12}}{c'_{22}} & 0 & 0 & 0 & \frac{1}{c'_{22}} & 0 \\ 0 & 0 & 0 & 0 & 0 & \frac{1}{c'_{44}} \\ \frac{c'^2_{12}}{c'_{22}} - c'_{11} & 0 & 0 & 0 & -\frac{c'_{12}}{c'_{22}} & 0 \\ 0 & 0 & 0 & -1 & 0 & 0 \\ 0 & 0 & -c'_{55} & 0 & 0 & 0 \end{bmatrix} \tag{6}$$

where primed elastic constants refer to the dislocation coordinate system. The eigenvalue problem gives the following analytical solutions:

$$\begin{aligned} p_1 &= \frac{1}{2}\left(\sqrt{2\lambda^2 - \eta} + \imath\sqrt{2\lambda^2 + \eta}\right) \\ p_2 &= \frac{1}{2}\left(-\sqrt{2\lambda^2 - \eta} + \imath\sqrt{2\lambda^2 + \eta}\right) \\ p_3 &= \imath\gamma \\ \boldsymbol{A}_\alpha &= \frac{1}{c'_{66}}\left[\frac{-(p_\alpha^2\gamma_1 + 1)}{(p_\alpha^2\gamma_1 - \gamma_0)}, \frac{p_\alpha(\gamma_0 + 1)}{(p_\alpha^2\gamma_1 - \gamma_0)}, 0\right] \\ \boldsymbol{A}_3 &= \left[0, 0, \imath/c'_{44}\right] \\ \boldsymbol{L}_\alpha &= [-p_\alpha, 1, 0], \quad \boldsymbol{L}_3 = [0, 0, -1] \end{aligned} \tag{7}$$

with $\alpha = (1, 2)$, $\eta = [\lambda^4\gamma_1 - (\gamma_0/\gamma_1)(\gamma_0 + 2)]$ and

$$\lambda^4 = \frac{c'_{11}}{c'_{22}}, \quad \gamma_0 = \frac{c'_{12}}{c'_{66}}, \quad \gamma_1 = \frac{c'_{22}}{c'_{66}}, \quad \gamma^2 = \frac{c'_{55}}{c'_{44}}. \tag{8}$$

Combining the above results and rearranging terms, the following equation is obtained:

$$C = \begin{cases} (\hat{\boldsymbol{d}}^* \cdot \hat{\boldsymbol{b}})^2 \left[\gamma(\hat{\boldsymbol{d}}^* \cdot \hat{\boldsymbol{n}})^2 + \gamma^{-1}(\hat{\boldsymbol{d}}^* \cdot [\hat{\boldsymbol{n}} \times \hat{\boldsymbol{b}}])^2\right] & \phi = 0 \\ (\hat{\boldsymbol{d}}^* \cdot \hat{\boldsymbol{b}})^2 \left[\zeta_1(\hat{\boldsymbol{d}}^* \cdot \hat{\boldsymbol{b}})^2 + \zeta_3(\hat{\boldsymbol{d}}^* \cdot \hat{\boldsymbol{n}})^2\right] + \zeta_2 (\hat{\boldsymbol{d}}^* \cdot \hat{\boldsymbol{n}})^4 & \phi = \dfrac{\pi}{2} \end{cases} \tag{9}$$

where

$$\begin{aligned} \zeta_i &= \frac{\mathcal{P}_i + \lambda^2 \mathcal{Q}_i}{\lambda^2 \mathcal{S}\sqrt{2\lambda^2 + \eta}}, \\ \mathcal{S} &= (2\gamma_0 + 4 - \gamma_1\eta), \\ \mathcal{P}_i &= \lambda^{4(i-1)}(\eta - 2\gamma_1\lambda^4)(\delta_{i,1} + \delta_{i,2}) + 2\lambda^4(2 + 4\gamma_0 + \gamma_1\eta)\delta_{i,3}, \\ \mathcal{Q}_i &= \lambda^{4(i-1)}(6 + 4\gamma_0 - \gamma_1\eta)(\delta_{i,1} + \delta_{i,2}) + (-\gamma_1)^{(i-2)}(n^2 - 4\lambda^4)(\delta_{i,2} \\ &\quad + \delta_{i,3}) + 6(\eta - 2\gamma_1\lambda^4)\delta_{i,3}. \end{aligned} \tag{10}$$

The chapeau (^) identifies unit vectors, $\hat{\boldsymbol{n}}$ is the vector normal to the slip plane, and ϕ is the angle between $\boldsymbol{l}$ and $\boldsymbol{b}$ (Figure 1a) alias dislocation character (equal to 0 for screw and $\pi/2$ for edge dislocations, respectively).

For any crystal symmetry, Equation (9) provides the contrast factor in a closed analytical form, as a function of the orientation of slip plane, Burgers and scattering vectors (i.e. corresponding Miller indices) and single-crystal elastic constants c_{ij}. The expression is valid for any dislocation lying on a diad axis with a further diad perpendicular to it; condition frequently met in a large variety of materials. Table 1 reports the values of λ^4, γ^2, γ_0, γ_1 in terms of elastic constants (in the crystal system as they can be usually found in the literature) for several representative examples.

3. The particular case of $\langle 1\bar{1}0\rangle\{001\}$ slip system

To illustrate the potentiality of Equation (9), the $\langle 1\bar{1}0\rangle\{001\}$ primary slip system in Fluorite-type structures is considered in more detail. As the crystal system is cubic, elastic constants can be conveniently written in terms of the elastic anisotropy (Zener ratio), $A_z = 2c_{44}/(c_{11} - c_{12})$, and the Poisson ratio $\nu = c_{12}/(c_{11} + c_{12})$. From Table 1

$$\begin{aligned} \lambda^4 &= \frac{A_z(1 - 2\nu) + 1}{2(1 - \nu)}, \quad \gamma_1 = \frac{2(1 - \nu)}{A_z(1 - 2\nu)}, \\ \gamma_0 &= \frac{2\nu}{A_z(1 - 2\nu)}, \quad \gamma^2 = \frac{1}{A_z}. \end{aligned} \tag{11}$$

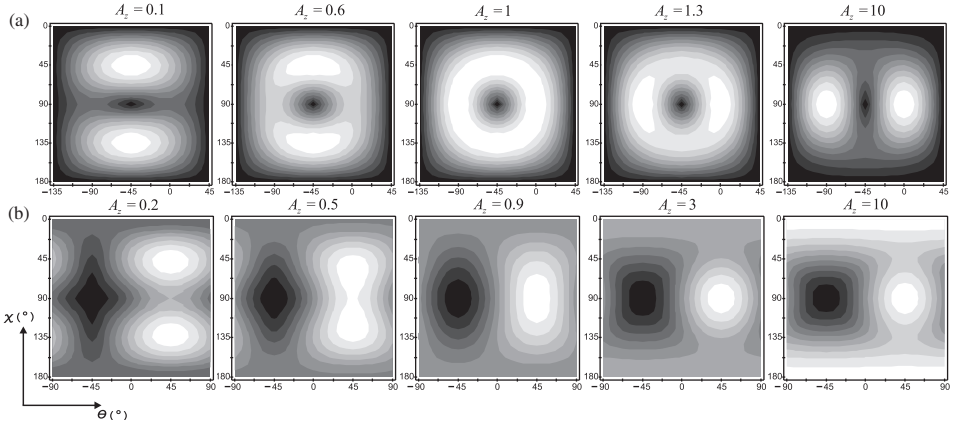

Figure 2. Contour maps of $\sqrt{C}$ as a function of the orientation of the scattering vector, for screw (a) and edge (b) dislocations, for different values of anisotropy ratio A_z. In (b), a fixed value $\nu = 0.3$ was used. (see Figure 1 and text for details).

The contrast factor in Equation (9) is then related to A_z and ν, through Equations (10) and (11).

To evaluate the dependence of the diffraction line broadening on A_z and ν, it is convenient to refer to $\sqrt{C}$ that can be shown proportional to the integral breadth (peak area divided by peak maximum intensity) of diffraction profiles [6].

Figure 2 shows the dependence of the line broadening anisotropy ($\sqrt{C}$ vs. $\hat{\boldsymbol{d}}^*$) of dislocations in the $\langle 1\bar{1}0\rangle\{001\}$ slip system, for several values of A_z. The dislocation line, $\mathbf{l} \parallel [1\bar{1}0]$ (Figure 1b), can be identified at the points $(\theta, \chi) = (-45^\circ, 90^\circ)$, for both screw and edge orientations, whereas the Burgers vector is at $(\theta, \chi) = (45^\circ, 90^\circ)$ in the edge case (Figure 2b). It can be seen that for any A_z, the diffraction line broadening is zero (darkest regions) either for ($\boldsymbol{d}^* \parallel \boldsymbol{l}$ or $\boldsymbol{d}^* \perp \boldsymbol{l}$) (Figure 2a) in the screw case, or for $\boldsymbol{d}^* \parallel \mathbf{l}$ (Figure 2b) in the edge case. This is equivalent to the invisibility criteria for screw/edge dislocations in transmission electron microscopy.

For screw orientation (Figure 2a), the main effect of A_z on the line broadening anisotropy is a $\pi/2$ rotation of the contour diagram around the center of the Figure 2a (dislocation line). As the A_z value crosses the isotropy condition, $A_z = 1$, the direction of maximum diffraction line broadening (lightest regions), undergoes a transition from $\boldsymbol{d}_1^* = [h\bar{h}h]$ $\{(\theta, \chi) = (-45^\circ, 45^\circ)\}$ to $\boldsymbol{d}_2^* = [h00]$ $\{(\theta, \chi) = (0^\circ, 90^\circ)\}$ Figure 3a). The threshold value ($A_z^s = 8/9$) is determined by the condition $\sqrt{C}(\boldsymbol{d}_1^*) = \sqrt{C}(\boldsymbol{d}_2^*)$. The inset of Figure 3(a) shows the difference, $\delta = |\sqrt{C}_{\text{ani}} - \sqrt{C}_{\text{iso}}|$, between $\sqrt{C}$ calculated along $\boldsymbol{d}_1^*$ and $\boldsymbol{d}_2^*$, respectively, by Equation (9) and within the isotropic elasticity approximation.

For edge dislocations, two parameters have to be considered: A_z and ν. Figure 2b shows the influence of A_z on the line broadening anisotropy for $\nu = 0.3$. By increasing A_z the maximum diffraction line broadening undergoes three transitions: from $\boldsymbol{d}_{1e}^* = [hhh]$ $\{(\theta, \chi) = (45^\circ, 45^\circ)\}$ to $\boldsymbol{d}_{2e}^* = [hh0]$ $\{(\theta, \chi) = (45^\circ, 90^\circ)\}$ and finally to $\boldsymbol{d}_{3e}^* = [00h]$ $\{(\theta, \chi) = (\theta, 0^\circ)\}$.

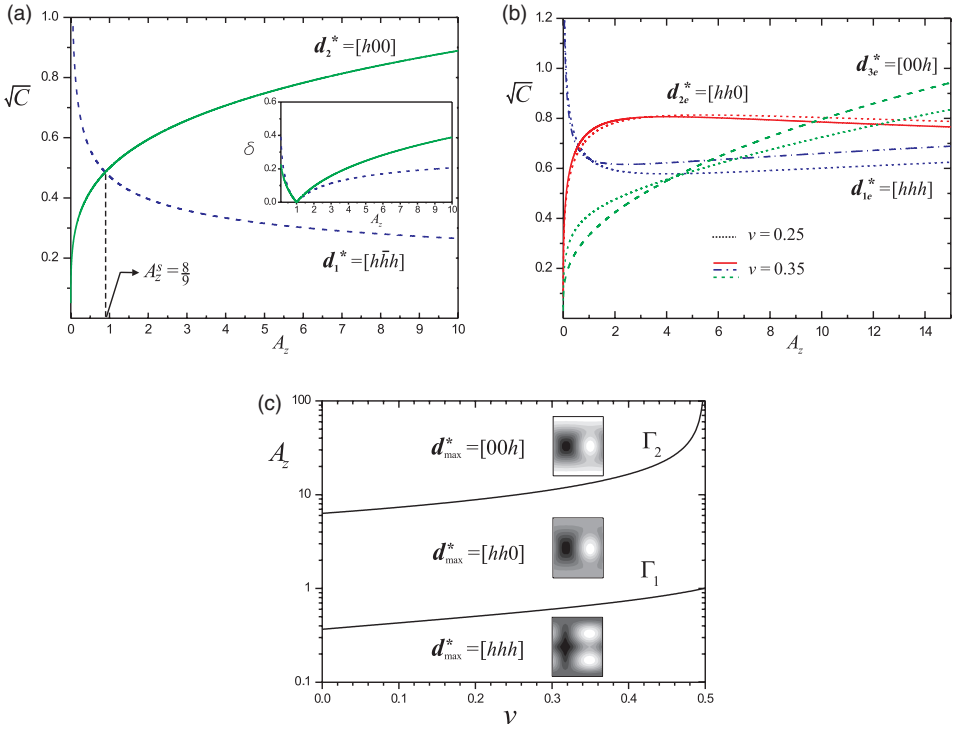

Figure 3. $\sqrt{C}$ as a function of A_z for some representative scattering vector directions for screw (a) and edge (b) dislocations. The *edge dislocation contrast diagram* is shown in (c) (see text for details).

Different values of ν have just a minor effect on $\sqrt{C}$, and therefore on the line broadening. This is illustrated in Figure 3b where $\sqrt{C}$ along $\{\boldsymbol{d}_{1e}^*, \boldsymbol{d}_{2e}^*, \boldsymbol{d}_{3e}^*\}$ is shown as a function of A_z for $\nu=0.25$ and for $\nu=0.35$.

In contrast to the screw case, transition values of A_z are no longer fixed points, but slowly-varying functions of the Poisson's Ratio. Figure 3c shows the curves Γ_1 and Γ_2 defining the maximum line broadening transitions for edge dislocations. They represent the set of critical points (ν^c, A_z^c) for which $\sqrt{C}(\boldsymbol{d}_{1e}^*)=\sqrt{C}(\boldsymbol{d}_{2e}^*)$ and $\sqrt{C}(\boldsymbol{d}_{2e}^*)=\sqrt{C}(\boldsymbol{d}_{3e}^*)$, respectively. As it can be seen, they delimit three regions in the (ν, A_z) plane: typical contour maps are shown for each region.

A similar analysis can easily be carried out for the other slip systems of Table 1 and for any other case of dislocations lying along a diad axis with a further diad perpendicular to it. Equation (9) can thus be used as a tool for studying dislocation line broadening effects in diffraction as well as for a quick calculation of corresponding contrast factors.

References

[1] E. Mittemeijer and P. Scardi, (eds.) *Diffraction Analysis of the Microstructure of Materials*, Springer-Verlag, Berlin, 2004.

[2] H.P. Klug and L.E. Alexander, *X-ray Diffraction Procedures for Polycrystalline and Amorphous Materials*, Wiley, New York, 1974.
[3] P. Scardi and M. Leoni, Acta Crystallogr., Sect. A.: Found. Crystallogr. 57 (2001) p.604.
[4] P. Scardi and M. Leoni, Acta Crystallogr., Sect. A.: Found. Crystallogr. A58 (2002) p.190.
[5] M. Wilkens, Phys. Status Solidi A 2 (1970) p.359.
[6] M. Krivoglaz, *X-ray Neutron Diffraction in Nonideal Crystals*, Springer-Verlag, Berlin, 1996.
[7] M. Wilkens, *Theoretical aspects of kinematical X-ray diffraction profiles from crystals containing dislocation distributions*, in *Fundamental Aspects of Dislocation Theory*, J.A. Simmons, R. de Wit and R. Bullough, (eds). National Bureau of Standards (NBS) U.S. Special Publication 317, II, Washington, D.C., 1970. p.1195.
[8] M. Wilkens, Phys. Status Solidi A. 104 (1987) p.K1.
[9] M. Leoni, J. Martinez-Garcia and P. Scardi, J. Appl. Crystallogr. 40 (2007) p.719.
[10] N.C. Popa, J. Appl. Crystallogr. 31 (1998) p.176.
[11] T. Ungár and G. Tichy, Phys. Status Solidi A 171 (1999) p.425.
[12] R. Kužel and P. Klimanek, J. Appl. Crystallogr. 21 (1988) p.363.
[13] J. Martinez-Garcia, M. Leoni and P. Scardi, Phys. Rev. B76 (2007) p.174117.
[14] P. Klimanek and R. Kužel, J. Appl. Crystallogr. 21 (1988) p.59.
[15] T.C.T. Ting, *Anisotropic Elasticity:Theory and Applications*, Oxford University Press, New York, 1996.